

## Article

# Silica Bifunctional Supports for the Direct Synthesis of H<sub>2</sub>O<sub>2</sub>: Optimization of Br/Acid Sites and Pd/Br Ratio

Gema Blanco-Brieva<sup>1</sup>, Frederique Desmedt<sup>2</sup>, Pierre Miquel<sup>2,†</sup>, Jose M. Campos-Martin<sup>1,\*</sup> and Jose L. G. Fierro<sup>1,‡</sup>

<sup>1</sup> Sustainable Energy and Chemistry Group, Instituto de Catálisis y Petroleoquímica, CSIC, Marie Curie, 2, Cantoblanco, 28049 Madrid, Spain; gblanco@icp.csic.es

<sup>2</sup> Solvay, Rue de Ransbeek, 310, B-1120 Brussels, Belgium; frederique.desmedt@solvay.com

\* Correspondence: j.m.campos@icp.csic.es

† Deceased (1982–2016).

‡ Deceased (1948–2020).

**Abstract:** We have studied the direct synthesis of hydrogen peroxide using a catalytic system consisting of palladium supported on silica bifunctionalized with sulfonic acid groups and bromide in the absence of acid and halide promoters in solution. Catalysts with several bromide substituents were employed in the catalyst synthesis. The prepared samples were characterized by TXRF, XPS, and hydrogen peroxide decomposition. Catalysts characterization indicated the presence of only palladium (II) species in all of the samples, with similar values for surface and bulk of Pd/Br atomic ratio. The catalysts were tested via direct synthesis, and all samples were able to produce hydrogen peroxide at 313 K and 5.0 MPa. The hydrogen peroxide yield and selectivity changed with the Pd/Br ratio. A decrease in the Pd/Br ratio increases the final hydrogen peroxide concentration, and the selectivity for H<sub>2</sub>O<sub>2</sub> reaches a maximum at a Pd/Br ratio around 0.16 and then decreases. However, the maximum hydrogen peroxide concentration and selectivity occur at slightly different Pd/Br ratios, i.e., resp. 0.4 vs. 0.16.

**Keywords:** direct synthesis; hydrogen peroxide; silica bifunctional supports; bromide



**Citation:** Blanco-Brieva, G.; Desmedt, F.; Miquel, P.; Campos-Martin, J.M.; Fierro, J.L.G. Silica Bifunctional Supports for the Direct Synthesis of H<sub>2</sub>O<sub>2</sub>: Optimization of Br/Acid Sites and Pd/Br Ratio. *Catalysts* **2022**, *12*, 796. <https://doi.org/10.3390/catal12070796>

Academic Editors: Federica Menegazzo and Sónia Carabineiro

Received: 6 June 2022

Accepted: 15 July 2022

Published: 19 July 2022

**Publisher's Note:** MDPI stays neutral with regard to jurisdictional claims in published maps and institutional affiliations.



**Copyright:** © 2022 by the authors. Licensee MDPI, Basel, Switzerland. This article is an open access article distributed under the terms and conditions of the Creative Commons Attribution (CC BY) license (<https://creativecommons.org/licenses/by/4.0/>).

## 1. Introduction

Hydrogen peroxide (H<sub>2</sub>O<sub>2</sub>), a green and selective chemical oxidant, is heavily used in industry. It decomposes to give water and oxygen as the only reaction products, which makes it very attractive from an environmental point of view as a strong oxidizing agent for many large-scale industrial applications [1,2]. Some of its most important uses in large-scale applications are bleaching cotton/textiles, wood pulp, paper, water purification, the treatment of wastewaters, and a wide variety of industrial wastes [3,4]. Due to its oxidizing nature, H<sub>2</sub>O<sub>2</sub> can oxidize a broad variety of inorganic and organic substrates in liquid-phase reactions, and is effective over the whole pH range with a high oxidation potential. Its main advantages over chlorine, chlorine-containing bleaches, and other oxidants that are used traditionally, such as sodium hypochlorite or sodium chlorite, are that it is suitable for continuous processing, and does not have high toxicity or effluent problems, and is noncorrosive. Given its multiple and varied ranges of applications, the method of H<sub>2</sub>O<sub>2</sub> production in the industry is of high interest.

A new research report by Global Market Insights Inc. determined that the Hydrogen Peroxide Market size is forecast to exceed \$6.2 billion by 2026 [5]. This increase can be mainly attributed to the field of chemical synthesis with the application of H<sub>2</sub>O<sub>2</sub> in the production of propylene oxide [6–9].

On an industrial scale, H<sub>2</sub>O<sub>2</sub> is manufactured mainly by the cyclic autooxidation of anthraquinones [10]. The process can only be considered to be economically viable on a relatively large scale. It should be noted that one of the major problems in this process is that

it requires large-scale infrastructure to produce highly concentrated  $\text{H}_2\text{O}_2$  (>70 wt.%  $\text{H}_2\text{O}_2$ ); however, dilute  $\text{H}_2\text{O}_2$  is required for many varied applications (>9 wt. %) [11]. For all these reasons, the development of a new, highly efficient, and smaller-scale manufacturing processes for  $\text{H}_2\text{O}_2$  would be of great commercial interest. A very attractive candidate is the production of  $\text{H}_2\text{O}_2$  by a direct, catalyzed reaction between hydrogen and oxygen. The infrastructure simply consumes less energy, and the process uses water or alcohols that are considered green solvents rather than organic substrates [10].

Direct synthesis (DS) is not a new process; it has been known since the beginning of the 20th century. The first patent was issued in 1914 by Henkel and Weber [12], as DS was considered to be the most promising alternative for  $\text{H}_2\text{O}_2$  production. Catalysts for DS are based on noble metals, and among them, palladium has exhibited the best results in the formation of  $\text{H}_2\text{O}_2$  in the liquid phase [13–16]. Although numerous patents have been issued since that date, no commercial process has been developed for this direct process. Much of the research on the direct synthesis of  $\text{H}_2\text{O}_2$  focuses on the design of the corresponding catalyst. Many studies are focused on the use of different metals or combinations of them [17–19] as well as the use of suitable supports to ensure that the unwanted reactions are minimal [3,20].

Some other very important aspects of these studies are to determine and subsequently rationalize the effect of different reaction conditions on the catalyst used [16] and to develop models focused on the study of the actual mechanism for a high optimization of the selectivity and production rate. The addition of stabilizers is normally needed to enhance hydrogen peroxide yields, and authors often use mineral acids in the reaction medium [21–23]. The presence of mineral acids in dissolution can negatively affect the stability of the catalyst due to the dissolution of the metallic active phase of the catalyst and the corrosion of the reactor materials. However, the acids are not only stabilizing, but it also seems that  $\text{H}^+$  ions can take part in  $\text{H}_2\text{O}_2$  formation [24]. The negative effect of the presence of free acid compounds in dissolution can be avoided through the use of catalytic supports functionalized with acidic groups [1,7,14,25–29].

However, the addition of acids is not enough to reach significant hydrogen peroxide production. Therefore, the addition of additives is necessary to inhibit the decomposition or hydrogenation of  $\text{H}_2\text{O}_2$ . Thus far, the best results were obtained by adding halide ions in the form of hydrohalic acids such as HBr or HCl, and salts such as KBr, KCl, or NaBr to the reaction medium [29–31]. Several studies have indicated that bromide is the best additive to enhance  $\text{H}_2\text{O}_2$  synthesis [21,32–34]. The effect of the added halides is difficult to rationalize, but it seems that they have a double effect blocking the sites of  $\text{H}_2\text{O}_2$  decomposition [35,36] and inhibiting the hydrogenation of  $\text{H}_2\text{O}_2$  by changing the surface charge of the catalyst [24,31,37,38]. The presence of halides in dissolution can produce problems of equipment corrosion and difficulties in separating them from the final  $\text{H}_2\text{O}_2$  product [28,39–42].

We recently showed that it is possible to use catalysts that contain both acidic and halide groups in the support structure [43] to reach a high hydrogen peroxide concentration (>4 wt.%). The final product has no acids or halides in dissolution and can be an attractive possibility for implementation at an industrial scale. However, optimization of the catalyst composition is necessary before application.

Here, we report a study of the optimization of a catalytic system consisting of supported palladium on commercial silica bifunctionalized with aryl sulfonic groups ( $\text{Si}-\text{O}-\text{C}_6\text{H}_4-\text{SO}_3\text{H}$ ) and aryl bromide groups ( $\text{Si}-\text{O}-\text{C}_6\text{H}_4-\text{Br}$ ) for the production of  $\text{H}_2\text{O}_2$  by a direct synthesis between  $\text{H}_2$  and  $\text{O}_2$  in non-acidic solutions or other additives outside the explosive limits of  $\text{H}_2/\text{O}_2$  mixtures.

## 2. Results and Discussion

### *Catalysts Characterization*

The chemical analysis, determined by Total reflection X-ray fluorescence (TXRF), of the supports indicates that the bromine loading is consistent with the nominal values; the

amount is lower for SO<sub>3</sub>H-Br-10 samples and increases for SO<sub>3</sub>H-Br-20, SO<sub>3</sub>H-Br-40, and SO<sub>3</sub>H-Br-50, in agreement with the nominal loading of brominated groups (Table 1). This trend is similar to the surface atomic ratio determined by X-ray photoelectron spectra (XPS) (Table 1). The sulfur surface concentration is similar for all catalysts. The surface atomic ratio of Br/S is consistent with that of the nominal brominated groups.

**Table 1.** Specifications, chemical composition determined by Total reflection X-ray fluorescence (TXRF), and surface atomic ratios of the support determined from X-ray photoelectron spectra (XPS) of silica supports.

Supports	% Brominated Phenyl Groups *	S (wt.%)	Br (wt.%)	Br/S Bulk (Atomic Ratio)	XPS		
					S/Si at	Br/Si at	Br/S at
SO <sub>3</sub> H-Br-10	10–20	2.15	1.69	0.31	0.060	0.009	0.15
SO <sub>3</sub> H-Br-20	20–30	2.22	2.28	0.41	0.061	0.017	0.28
SO <sub>3</sub> H-Br-40	40–50	2.18	3.50	0.64	0.062	0.027	0.44
SO <sub>3</sub> H-Br-50	50–60	2.20	6.89	1.26	0.059	0.059	1.00

\* Nominal brominated phenyl groups to total groups incorporated into the silica provided by Silicycle Company.

Several catalysts with several Pd/Br ratios were prepared by ionic exchange of palladium salts with sulfonic groups employing different silica supports, having in mind that the interaction of palladium–bromine would be less efficient in catalysts with anchored Br species with respect to adding these Br species in solution, it is reasonable to think that a higher amount of Br is necessary for the heterogeneous samples. The chemical analysis of the samples depicted in Table 2. shows that the concentration of Br is practically the same in the catalysts with respect to the commercial support counterparts. In all catalysts, the amount of palladium incorporated is very similar and approximately 1.7 wt.%. The surface concentration determined by XPS follows similar trends. The atomic ratio Br/Pd determined by XPS is similar to the bulk ratios determined by chemical analysis.

**Table 2.** Chemical composition determined by Total reflection X-ray fluorescence (TXRF) and surface atomic ratios of the support determined from X-ray photoelectron spectra (XPS) of the prepared catalysts.

Catalysts	Br (wt.%)	Pd (wt.%)	Pd/Br Bulk (Atomic Ratio)	XPS					
				S/Si at	Br/Si at	Pd/Si at	Br/S at	Pd/S at	Pd/Br at
Pd/SO <sub>3</sub> H-Br-10	1.33	1.73	0.98	0.064	0.009	0.008	0.14	0.13	0.89
Pd/SO <sub>3</sub> H-Br-20	2.14	1.70	0.60	0.062	0.017	0.009	0.27	0.15	0.53
Pd/SO <sub>3</sub> H-Br-40	3.30	1.76	0.40	0.068	0.024	0.010	0.35	0.15	0.42
Pd/SO <sub>3</sub> H-Br-50	6.76	1.75	0.19	0.067	0.058	0.008	0.87	0.13	0.16

The chemical state of palladium was determined from the binding energy of the Pd 3d<sub>5/2</sub> peak of the XPS spectra. All samples showed the presence of two palladium (II) species (Figure 1 and Table 3); a minor component at 336.4 eV is typical of a PdO-supported species, and the main component at higher binding energy (338.1 eV) [14,26,27,43] can be attributed to an oxidized palladium species interacting with sulfonic groups. This point is important because a catalyst with a higher amount of Pd(II) species interacting with the acid groups (high BE) gives higher selectivity to H<sub>2</sub>O<sub>2</sub>, as was observed in our previous studies [7,14,25–27,43]. Has not been detected reduced palladium species, as expected because all samples were analyzed without any reduction treatment. Some XPS measurements of the used catalysts were made, and the palladium signal had several components that indicated the presence of a mixture of metallic palladium and oxidized species. There are several components in the reaction system; excess oxygen (approximately 46.4%) and methanol have an opposite effect on the palladium oxidation state for a reaction at 313 K. However, the treatment

of the samples after use in the reaction, for example, washing and drying, makes it very difficult to obtain an accurate ratio of the true oxidized/reduced catalyst species in the reaction media.

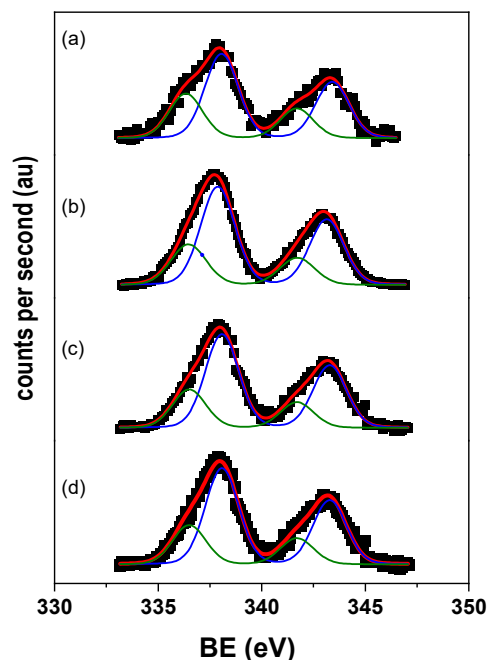


**Figure 1.** Pd  $3d_{5/2}$  core-level spectra of catalysts determined by XPS for fresh catalysts: (a) Pd/SO<sub>3</sub>H-Br-10, (b) Pd/SO<sub>3</sub>H-Br-20, (c) Pd/SO<sub>3</sub>H-Br-40, and (d) Pd/SO<sub>3</sub>H-Br-50.

**Table 3.** Binding energy (eV) of Pd  $3d_{5/2}$  core levels for prepared catalysts (the relative proportion of each peak is given in parenthesis).

Catalysts	BE Pd $3d_{5/2}$ (eV)
Pd/SO <sub>3</sub> H-Br-10	336.3 (40)
	338.1 (60)
Pd/SO <sub>3</sub> H-Br-20	336.4 (35)
	338.0 (65)
Pd/SO <sub>3</sub> H-Br-40	336.5 (29)
	338.1 (71)
Pd/SO <sub>3</sub> H-Br-50	336.7 (30)
	338.0 (70)

XRD profiles of palladium catalysts supported on sulfonic acid-functionalized silica (1.92 wt.% Pd) showed only a broad peak due to silica substrate, but no diffraction lines of Pd species were observed, indicating that the size of palladium particles is very small, or non-crystalline (see Figure S1, Supplementary Material).

Also, the structure and morphology of the catalysts and samples were analyzed by TEM, being difficult to measure in transmission mode, mainly due to the presence of oxidized small particles. It was, therefore, necessary to analyze in STEM mode, which magnifies the contrast between the support and the palladium species. All samples showed a homogeneous distribution of Pd particles with a size around 1–4 nm (Figure 2). These results are in agreement with our previous study [14]; as a consequence, the Pd/Br ratio does not affect the Pd crystallite size.

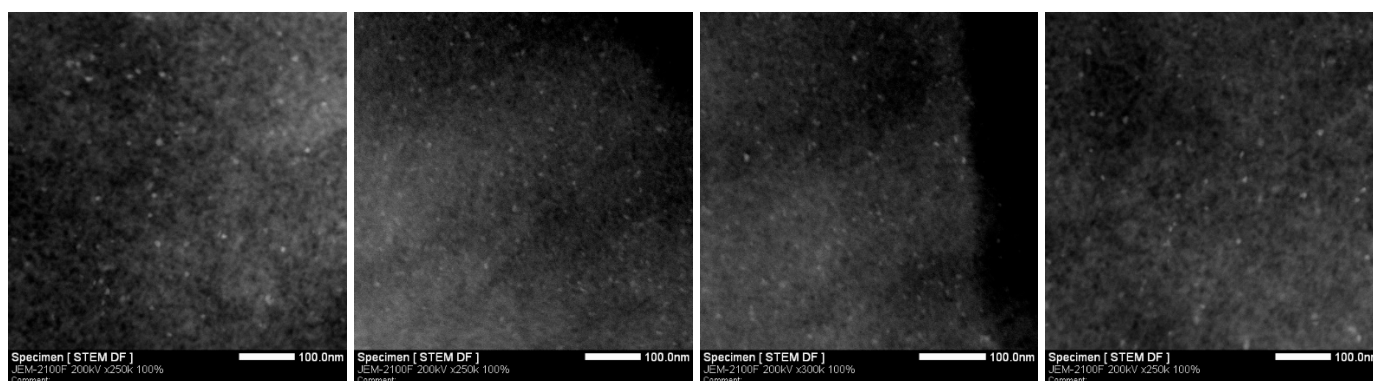


**Figure 2.** STEM images of the samples Pd/SO<sub>3</sub>H-Br-10, Pd/SO<sub>3</sub>H-Br-20, Pd/SO<sub>3</sub>H-Br-40, and Pd/SO<sub>3</sub>H-Br-50.

Previous works showed that the interaction of bromine and palladium affects the palladium catalysts' ability to decompose the hydrogen peroxide [43]. The catalysts employed as prepared without any reduction treatment were tested with a 10 wt.% of hydrogen peroxide at 40 °C, and all catalysts were active in the decomposition reaction of H<sub>2</sub>O<sub>2</sub> (Figure 3). The highest decomposition rate was reached with the catalyst Pd-SO<sub>3</sub>H-Br-10, while the decomposition decreased with the increase in the amount of bromide in the catalyst (Table 2), Pd-SO<sub>3</sub>H-Br-50 catalysts showed the lowest decomposition extent (Figure 3). This observation can be related to the fact that the higher amount of brominated groups in the support produces a higher interaction with the palladium species present in the catalyst reduces the hydrogen peroxide decomposition ability of the catalyst. The Br species blocks the unsaturated sites, and this site favors the decomposition of H<sub>2</sub>O<sub>2</sub> [44]. Thus, the lower decomposition rate is due to a higher Pd-Br interaction. On the other hand, the block of unsaturated sites will decrease the water formation during direct hydrogen peroxide reaction because these unsaturated sites favor water formation [44]. As a result, this simple test can be used to sort the catalytic behavior of the catalysts in a direct synthesis reaction.

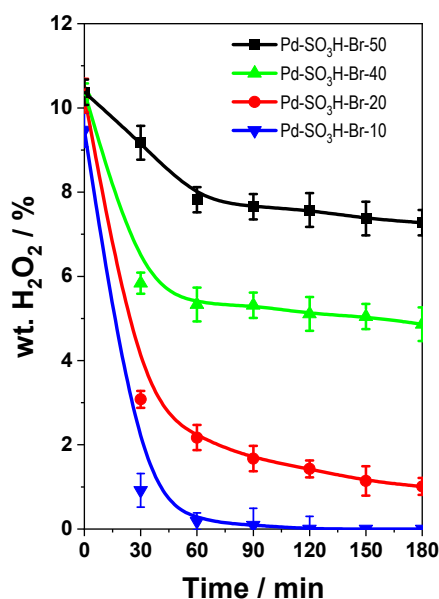


**Figure 3.** Stability test at 313 K for catalysts prepared from commercial silica supports.

These catalysts, employed as prepared without any reduction treatment, were tested in the direct synthesis of H<sub>2</sub>O<sub>2</sub> without the addition of any bromine compound in dissolution (320 g methanol, P = 5.0 MPa, T = 313 K, total flow: 5300 mL(STP) min<sup>-1</sup>, 3.6% H<sub>2</sub>: 55% O<sub>2</sub>: 41.4 N<sub>2</sub>). Catalysts were employed as prepared without any reduction treatment. As

the catalyst contained a different palladium loading, the amount of catalyst added to the reactor was appropriately selected to keep the quantity of palladium inside the reactor constant in all experiments.

The liquid samples at the end of the reaction were analyzed by ICP-OES and by ionic chromatography for possible leaching of bromide or palladium species. No palladium was detected by ICP-OES ( $<0.1$  Pd ppm), and no bromide ions in dissolution were detected ( $<0.5$  ppb). The absence of palladium leaching was observed in all of our previous work where the acid promoter was incorporated in the heterogeneous catalyst [34]. This behavior is different when acidic and bromide promoters are present in dissolution (NaBr +  $H_3PO_4$ ) [29]; under these conditions, the authors found the partial leaching of palladium.

For all catalysts tested the hydrogen consumption was high ( $>90\%$ ) and similar, however, small differences have been detected among the samples, and the hydrogen consumption is slightly smaller as small as the Pd/Br.  $H_2O_2$  formation was detected for all catalysts tested with significant amounts of  $H_2O_2$  ( $>4$  wt.%) obtained after 3h of reaction (Figure 4). Furthermore, these catalytic systems clearly had more sustainable profiles (absence of additives in solution). The amount of bromine present in the catalysts (Table 2) seemed to have an important effect on the hydrogen peroxide concentration and selectivity of the  $H_2O_2$  profiles (Figure 4) which indicates that Br on the support surface interacts with Pd sites. The hydrogen peroxide concentration obtained increased as the Br content on the support, reached a maximum for Pd/SO<sub>3</sub>H-Br-40, and decreased with the Pd/SO<sub>3</sub>H-Br-50 catalysts.

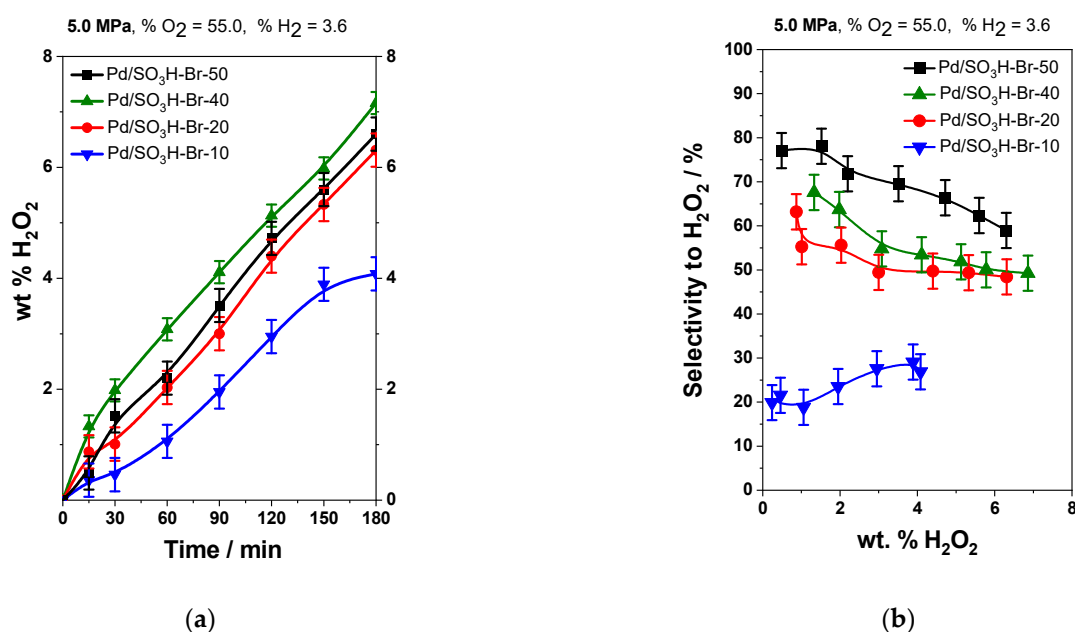


**Figure 4.** (a)  $H_2O_2$  concentration profiles versus time at 313 K and 5.0 MPa; (b) Influence of the amount of bromide in the supports on the selectivity for  $H_2O_2$ .

The selectivity is higher at low hydrogen peroxide concentration, for instance, around 79% for Pd/SO<sub>3</sub>H-Br-50, and decreases with the concentration of hydrogen peroxide (Figure 4); the selectivity tends to stabilize for hydrogen peroxide concentration higher than 5 wt.% around 50–60% depending on the catalysts employed. The selectivity of the  $H_2O_2$  profiles shows an increase in the selectivity as the Br content determined by chemical analysis, as shown in Table 2, increased: Pd/SO<sub>3</sub>H-Br-10 < Pd/SO<sub>3</sub>H-Br-20 < Pd/SO<sub>3</sub>H-Br-40 < Pd/SO<sub>3</sub>H-Br-50 (Figure 4). This behavior may be related to the interaction of the Br present on the surface with the palladium. The supports with low Br contents have lower interaction points, which increase as the Br content increases. The

differences in the interaction were previously observed in the hydrogen peroxide stability experiments (Figure 3).

Density functional theory (DFT) studies of the  $H_2-O_2$  reaction on Pd catalysts distinguish two types of sites: more unsaturated sites, such as corners or edges, and more saturated sites, such as a (111) face [44]. The energy profiles of the  $H_2 + O_2$  reaction suggest that  $H_2O_2$  would be smoothly produced at more saturated sites, whereas the formation of  $H_2O$  and the decomposition of  $H_2O_2$  would be preferred at more unsaturated sites. Br blocks the unsaturated sites and reduces secondary reactions because the adsorption energy of bromide and protons is higher than that of  $H_2$  and  $O_2$  [44]. This role of the Br content can explain the decrease in the hydrogen peroxide concentration in Pd/SO<sub>3</sub>H-Br-50 with respect to Pd/SO<sub>3</sub>H-Br-40, despite the higher selectivity of the former. The presence of a greater relative amount of Br leads to a decrease in the activity of Pd because the Br blocks some surface sites, inhibiting  $H_2$  and  $O_2$  adsorption, in agreement with the observation of the slight decrease of hydrogen conversion with the decrease in the Pd/Br ratio.

Based on these results, we prepared an additional catalyst with the SO<sub>3</sub>H-Br-50 support but with a lower amount of palladium (1.11 wt.%). In this catalyst, the Pd/Br ratio was smaller than 0.12. This catalyst showed lower hydrogen peroxide formation in comparison with the Pd/SO<sub>3</sub>H-Br-50 and Pd/SO<sub>3</sub>H-Br-40 catalysts, and selectivity for hydrogen peroxide was lower than that of the Pd/SO<sub>3</sub>H-Br-50 catalyst and similar to that of the Pd/SO<sub>3</sub>H-Br-40 catalyst. These results newly indicate a tremendous effect of the Pd/Br ratio on the catalytic behavior of hydrogen peroxide direct synthesis [14,43]. The optimal values of Pd/Br when the precursor is in solution are different with respect to the samples where Br is incorporated in dissolution. This is because, in the homogeneous systems, all Br species are available to interact with the palladium species, while in the case of the heterogeneous samples, some Br moieties are close to palladium species and others are farther than is reasonable to think that a higher amount of bromine is needed in heterogeneous samples. The optimal value of Pd/Br is between 0.40 and 0.16. A higher Pd/Br ratio yields a higher activity and a slightly higher concentration of hydrogen peroxide but lower hydrogen peroxide selectivity, while a lower Pd/Br ratio shows the opposite trend.

### 3. Materials and Methods

#### 3.1. Materials

The supports used for palladium catalyst synthesis were the following: SiliaBond<sup>®</sup>Tosic Acid & 10, 20, 40, and 50% Br phenyl bromide groups (aryl sulfonic groups and aryl bromide groups). All these supports were purchased from Silicycle Inc., and with the exception of the SiliaBond<sup>®</sup>Tosic, the other ones that contain Br were prepared specifically for our group and are not commercial ones. The palladium precursor was Pd(II) acetate (45.9–48.4 %Pd) and was purchased from Johnson Matthey.

#### 3.2. Catalysts Preparation

A suspension of bifunctionalized commercial silica with aryl sulfonic groups (Si-C<sub>6</sub>H<sub>4</sub>-SO<sub>3</sub>H) and aryl bromide groups purchased from Silicycle Inc. (10 g) was prepared in acetone (125 mL) and maintained while stirring for 1 h at room temperature. A Pd(II) acetate (Johnson Matthey) solution in 50 mL of acetone was added dropwise to the suspension. After 1 h of contact at RT, the solid was filtered off, washed with acetone, and dried at 333 K for 1 h.

#### 3.3. Catalyst Characterization

##### 3.3.1. TXRF

Total reflection X-ray fluorescence (TXRF) analysis was performed with a benchtop S2 PicoFox TXRF spectrometer from Bruker Nano GmbH (Berlin, Germany) equipped with a molybdenum X-ray source working at 50 kV and 600  $\mu$ A, a multilayer monochromator with 80% reflectivity at 17.5 keV (Mo K $\alpha$ ), and an XFlash SDD detector with an effective area of 30 mm<sup>2</sup>; the energy resolution was greater than 150 eV for Mn K $\alpha$ . The fine beam is

reflected off a polished sample carrier at a very small angle ( $<0.1^\circ$ ). Because the intensity of incident X-ray beams is almost entirely reflected, the remaining intensity penetrates only a few nanometers (approximately 10–15 nm) in the sample.

### 3.3.2. XRD

X-ray diffraction profiles of samples were recorded with an X'Pert Pro PANalytical diffractometer equipped with a  $\text{CuK}\alpha$  radiation source ( $\lambda = 0.15418$  nm) and X'Celerator detector based on RTMS (real-time multiple-strip) technology. The samples were ground and placed on a stainless steel plate. The diffraction patterns were recorded in steps over a range of Bragg angles ( $2\theta$ ) between  $4^\circ$  and  $90^\circ$  at a scanning rate of  $0.02^\circ$  per step and an accumulation time of 50 s. Diffractograms were analyzed with X'Pert HighScore Plus software.

### 3.3.3. TEM

Transmission Electron Microscopy (TEM) and Scanning Transmission Electron Microscopy (STEM) images of the catalysts were obtained using a 200 kV field emission gun transmission electron microscope (JEOL 2100F) and equipped with an EDX X-Max 80 spectrometer (Oxford Instruments). Specimens were prepared by dropping the suspension of the sample in ethanol on a copper grid covered by a carbon film.

### 3.3.4. XPS

X-ray photoelectron spectra (XPS) were acquired with a VG Escalab 200R spectrometer equipped with a hemispherical electron analyzer and an  $\text{Mg K}\alpha$  ( $h\nu = 1253.6$  eV) non-monochromatic X-ray source. The samples were degassed in the pretreatment chamber at room temperature for 1 h before being transferred into the instrument's ultrahigh vacuum analysis chamber. The Si 2p, O 1s, S 2p, Br 1s, and C 1s signals were scanned several times at a pass energy of 20 eV to obtain good signal-to-noise ratios and good resolution. The binding energies (BE) were referenced to the BE of the C 1s signal at 284.9 eV. The invariance of the peak shapes and widths at the beginning and end of the analyses indicated a constant charge throughout the measurements. The peaks were fitted by a nonlinear least-squares fitting method using a properly weighted sum of the Lorentzian and Gaussian component curves after background subtraction.

## 3.4. Hydrogen Peroxide Solution Stability

The stability test for the different prepared catalysts employed as prepared without any reduction treatment was conducted by the following protocol: 25.52 g of high purity 30 wt.%  $\text{H}_2\text{O}_2$  solution in water (supplied by Solvay) and 53.48 g of methanol were mixed in a glass reactor to obtain an  $\text{H}_2\text{O}_2$  solution of 10 wt.%, a value close to the maximum concentration reached in the reaction. This solution was heated at a temperature of 313 K while stirring, and when this temperature was stable, a sample was taken (coded as sample 0). The amount of catalyst necessary to load 0.062 g of Pd in the reactor was then added to the mixture, and a sample was taken every 30 min for a period of 3 h.

## 3.5. Hydrogen Peroxide Direct Synthesis

Catalysts were tested in the direct synthesis of  $\text{H}_2\text{O}_2$  by introducing the same amount of palladium in the reactor and modifying the amount of catalyst present in the reactor in semi-batch mode. The catalysts were employed as prepared without any reduction treatment.

In the system, the liquid was kept inside the 1L reactor (Autoclave Engineers) throughout the experiment while a continuous gas flow was fed, and the pressure in the reactor was held constant using a pressure controller on the autoclave. Then, 320 g of MeOH was added to the reactor, and the system was pressurized under  $\text{N}_2$  flow at a reaction pressure of 5.0 MPa and heated to 313 K. Then,  $\text{O}_2$  and  $\text{H}_2$  were added successively without stirring to prevent the reaction from the beginning. The total gas flow was 5300 mL (STP)·min<sup>-1</sup>, and the molar concentrations of the gases were as follows: 3.6%  $\text{H}_2$ ; 46.4%  $\text{O}_2$ ; and 50.0%

N<sub>2</sub> (outside flammability limits). When the system was stable, the reaction was started by stirring the mixture (1500 rpm). An online gas chromatograph (Varian CP-4900 micro GC) was used to determine the consumption of hydrogen. H<sub>2</sub>O<sub>2</sub> was determined by standard titration with potassium permanganate with 2 M sulfuric acid solution (reduction of permanganate with H<sub>2</sub>O<sub>2</sub> in acidic solutions), and the water concentrations were determined by volumetric Karl Fisher titration. The selectivity was calculated based on the concentrations of H<sub>2</sub>O<sub>2</sub> and water formed during the reaction.

#### 4. Conclusions

We present a catalytic system consisting of supported palladium on silica bifunctionalized with sulfonic acid groups and bromide. The characterization of the catalysts indicated the presence of only the palladium (II) species in all of the samples, with similar values for surface and bulk of Pd/Br atomic ratio. This system produces hydrogen peroxide at high concentrations (>4 wt.%) by the direct synthesis in the absence of acid and halide promoters in dissolution. The prepared catalysts employed as prepared without any reduction treatment can produce hydrogen peroxide, but the hydrogen peroxide yield and selectivity change with the Br contents of the catalysts. A careful study indicates that the yield and selectivity of the catalyst are more related to the Pd/Br ratio. A decrease in the Pd/Br ratio increases the final hydrogen peroxide concentration, and the selectivity to H<sub>2</sub>O<sub>2</sub> reaches a maximum and then decreases. However, the maximum hydrogen peroxide concentration and selectivity occur at slightly different Pd/Br ratios. It is necessary to select a value between the maximum hydrogen peroxide concentration and selectivity.

The hydrogen peroxide decomposition test can be used to sort the catalytic behavior of the catalysts in a direct synthesis reaction. This is because it is a test to evaluate the block of the unsaturated sites responsible for the H<sub>2</sub>O<sub>2</sub> decomposition and water formation during the direct hydrogen peroxide synthesis.

**Supplementary Materials:** The following supporting information can be downloaded at: <https://www.mdpi.com/article/10.3390/catal12070796/s1>, Figure S1: XRD profiles of the catalysts prepared.

**Author Contributions:** Conceptualization, J.M.C.-M. and J.L.G.F.; formal analysis, G.B.-B., J.M.C.-M., J.L.G.F., F.D. and P.M.; investigation, G.B.-B.; writing—original draft preparation, G.B.-B.; writing—review and editing, J.M.C.-M., J.L.G.F., F.D. and P.M.; J.M.C.-M., J.L.G.F., F.D. and P.M.; funding acquisition. All authors have read and agreed to the published version of the manuscript.

**Funding:** This research was funded by SOLVAY (Brussels).

**Institutional Review Board Statement:** Not applicable.

**Informed Consent Statement:** Not applicable.

**Data Availability Statement:** Not applicable.

**Conflicts of Interest:** There are no conflicts of interest to declare.

**Sample Availability:** Samples of the different catalysts are available from the authors.

#### References

1. Campos-Martin, J.M.; Blanco-Brieva, G.; Fierro, J.L.G. Hydrogen peroxide synthesis: An Outlook beyond the Anthraquinone Process. *Angew. Chem. Int. Ed.* **2006**, *45*, 6962–6984. [[CrossRef](#)] [[PubMed](#)]
2. Wilson, N.M.; Bregante, D.T.; Priyadarshini, P.; Flaherty, D.W. Production and use of H<sub>2</sub>O<sub>2</sub> for atom-efficient functionalization of hydrocarbons and small molecules. In *Catalysis*; The Royal Society of Chemistry: London, UK, 2017; Volume 29, pp. 122–212.
3. Kim, H.; Ross, M.; Kornienko, N.; Zhang, L.; Guo, J.; Yang, P.; McCloskey, B. Efficient hydrogen peroxide generation using reduced graphene oxide-based oxygen reduction electrocatalysts. *Nat. Catal.* **2018**, *1*, 282–290. [[CrossRef](#)]
4. Goor, G.; Glenneberg, J.; Jacobi, S. Hydrogen peroxide. In *Ullmann's Encyclopedia of Industrial Chemistry*; Verlag Chemie: Hoboken, NJ, USA, 1991.
5. Kiran Pulidindi, S.M. *Hydrogen Peroxide Market Size Worth over \$6.2 Billion by 2026*; Global Market Insights: Selbyville, DE, USA, 2020.
6. Lin, M.; Xia, C.; Zhu, B.; Li, H.; Shu, X. Green and efficient epoxidation of propylene with hydrogen peroxide (HPPO process) catalyzed by hollow TS-1 zeolite: A 1.0kt/a pilot-scale study. *Chem. Eng. J.* **2016**, *295*, 370–375. [[CrossRef](#)]

7. Blanco-Brieva, G.; Capel-Sanchez, M.C.; de Frutos, M.P.; Padilla-Polo, A.; Campos-Martin, J.M.; Fierro, J.L.G. New two-step process for propene oxide production (HPPO) based on the direct synthesis of hydrogen peroxide. *Ind. Eng. Chem. Res.* **2008**, *47*, 8011–8015. [[CrossRef](#)]
8. Wang, Y.; Li, H.; Liu, W.; Lin, Y.; Han, X.; Wang, Z. Effect of TS-1 treatment by mixed alkaline on propylene epoxidation. *Trans. Tianjin Univ.* **2018**, *24*, 25–31. [[CrossRef](#)]
9. Xu, L.; Ding, J.; Yang, Y.; Wu, P. Distinctions of hydroxylamine formation and decomposition in cyclohexanone ammoxidation over microporous titanosilicates. *J. Catal.* **2014**, *309*, 1–10. [[CrossRef](#)]
10. Ranganathan, S.; Sieber, V. Recent advances in the direct synthesis of hydrogen peroxide using chemical catalysis—A review. *Catalysts* **2018**, *8*, 379. [[CrossRef](#)]
11. Yang, S.; Verdaguer-Casadevall, A.; Arnarson, L.; Silvioli, L.; Čolić, V.; Frydendal, R.; Rossmeisl, J.; Chorkendorff, I.; Stephens, I.E.L. Toward the decentralized electrochemical production of H<sub>2</sub>O<sub>2</sub>: A focus on the catalysis. *ACS Catal.* **2018**, *8*, 4064–4081. [[CrossRef](#)]
12. Hugo Henkel, W.W. Manufacture of hydrogen peroxide. U.S. Patent US1108752A, 25 August 1914.
13. Biasi, P.; García-Serna, J.; Bittante, A.; Salmi, T. Direct synthesis of hydrogen peroxide in water in a continuous trickle bed reactor optimized to maximize productivity. *Green Chem.* **2013**, *15*, 2502–2513. [[CrossRef](#)]
14. Blanco-Brieva, G.; de Frutos Escrig, M.P.; Campos-Martin, J.M.; Fierro, J.L.G. Direct synthesis of hydrogen peroxide on palladium catalyst supported on sulfonic acid-functionalized silica. *Green Chem.* **2010**, *12*, 1163–1166. [[CrossRef](#)]
15. Edwards, J.K.; Hutchings, G.J. Palladium and gold–palladium catalysts for the direct synthesis of hydrogen peroxide. *Angew. Chem. Int. Ed.* **2008**, *47*, 9192–9198. [[CrossRef](#)] [[PubMed](#)]
16. Dittmeyer, R.; Grunwaldt, J.D.; Pashkova, A. A review of catalyst performance and novel reaction engineering concepts in direct synthesis of hydrogen peroxide. *Catal. Today* **2015**, *248*, 149–159. [[CrossRef](#)]
17. Solsona, B.E.; Edwards, J.K.; Landon, P.; Carley, A.F.; Herzing, A.; Kiely, C.J.; Hutchings, G.J. Direct synthesis of hydrogen peroxide from H<sub>2</sub> and O<sub>2</sub> Using Al<sub>2</sub>O<sub>3</sub> supported Au–Pd catalysts. *Chem. Mater.* **2006**, *18*, 2689–2695. [[CrossRef](#)]
18. Wilson, N.M.; Pan, Y.-T.; Shao, Y.-T.; Zuo, J.-M.; Yang, H.; Flaherty, D.W. Direct synthesis of H<sub>2</sub>O<sub>2</sub> on AgPt octahedra: The importance of Ag–Pt coordination for high H<sub>2</sub>O<sub>2</sub> selectivity. *ACS Catal.* **2018**, *8*, 2880–2889. [[CrossRef](#)]
19. Wilson, N.M.; Priyadarshini, P.; Kunz, S.; Flaherty, D.W. Direct synthesis of H<sub>2</sub>O<sub>2</sub> on Pd and AuPd<sub>1</sub> clusters: Understanding the effects of alloying Pd with Au. *J. Catal.* **2018**, *357*, 163–175. [[CrossRef](#)]
20. Vu, H.T.T.; Vo, V.L.N.; Chung, Y.-M. Direct synthesis of hydrogen peroxide over palladium catalysts supported on glucose-derived amorphous carbons. *Korean J. Chem. Eng.* **2021**, *38*, 1139–1148. [[CrossRef](#)]
21. Samanta, C.; Choudhary, V.R. Direct oxidation of H<sub>2</sub> to H<sub>2</sub>O<sub>2</sub> over Pd/Ga<sub>2</sub>O<sub>3</sub> catalyst under ambient conditions: Influence of halide ions added to the catalyst or reaction medium. *Appl. Catal. A: Gen.* **2007**, *326*, 28–36. [[CrossRef](#)]
22. Choudhary, V.R.; Ingole, Y.V.; Samanta, C.; Jana, P. Direct oxidation of hydrogen to hydrogen peroxide over Pd (or PdO)/Al<sub>2</sub>O<sub>3</sub> in aqueous reaction medium: influence of different acids and halide anions in reaction medium on formation and destruction of H<sub>2</sub>O<sub>2</sub>. *Ind. Eng. Chem. Res.* **2007**, *46*, 8566–8573. [[CrossRef](#)]
23. Burch, R.; Ellis, P. An investigation of alternative catalytic approaches for the direct synthesis of hydrogen peroxide from hydrogen and oxygen. *Appl. Catal. B-Environ.* **2003**, *42*, 203–211. [[CrossRef](#)]
24. Wilson, N.M.; Flaherty, D.W. Mechanism for the direct synthesis of H<sub>2</sub>O<sub>2</sub> on Pd clusters: Heterolytic reaction pathways at the liquid–solid interface. *J. Am. Chem. Soc.* **2016**, *138*, 574–586. [[CrossRef](#)]
25. Blanco-Brieva, G.; Cano-Serrano, E.; Campos-Martin, J.M.; Fierro, J.L.G. Direct synthesis of hydrogen peroxide solution with palladium-loaded sulfonic acid polystyrene resins. *Chem. Commun.* **2004**, *10*, 1184–1185. [[CrossRef](#)]
26. Blanco-Brieva, G.; Montiel-Argaiz, M.; Desmedt, F.; Miquel, P.; Campos-Martin, J.M.; Fierro, J.L.G. Direct synthesis of hydrogen peroxide with no ionic halides in solution. *RSC Adv.* **2016**, *6*, 99291–99296. [[CrossRef](#)]
27. Brieva, G.; Montiel, M.; Desmedt, F.; Miquel, P.; Campos-Martin, J.; Fierro, J. Effect of the acidity of the groups of functionalized silicas on the direct synthesis of H<sub>2</sub>O<sub>2</sub>. *Top. Catal.* **2017**, *60*, 1151–1155. [[CrossRef](#)]
28. Sterchele, S.; Biasi, P.; Centomo, P.; Campestrini, S.; Shchukarev, A.; Rautio, A.-R.; Mikkola, J.-P.; Salmi, T.; Zecca, M. The effect of the metal precursor-reduction with hydrogen on a library of bimetallic Pd–Au and Pd–Pt catalysts for the direct synthesis of H<sub>2</sub>O<sub>2</sub>. *Catal. Today* **2015**, *248*, 40–47. [[CrossRef](#)]
29. Biasi, P.; Mikkola, J.-P.; Sterchele, S.; Salmi, T.; Gemo, N.; Shchukarev, A.; Centomo, P.; Zecca, M.; Canu, P.; Rautio, A.-R.; et al. Revealing the role of bromide in the H<sub>2</sub>O<sub>2</sub> direct synthesis with the catalyst wet pretreatment method (CWPM). *AIChE J.* **2017**, *63*, 32–42. [[CrossRef](#)]
30. Centomo, P.; Meneghini, C.; Sterchele, S.; Trapananti, A.; Aquilanti, G.; Zecca, M. In situ X-ray absorption fine structure spectroscopy of a palladium catalyst for the direct synthesis of hydrogen peroxide: Leaching and reduction of the metal phase in the presence of bromide ions. *ChemCatChem* **2015**, *7*, 3712–3718. [[CrossRef](#)]
31. Priyadarshini, P.; Ricciardulli, T.; Adams, J.S.; Yun, Y.S.; Flaherty, D.W. Effects of bromide adsorption on the direct synthesis of H<sub>2</sub>O<sub>2</sub> on Pd nanoparticles: Formation rates, selectivities, and apparent barriers at steady-state. *J. Catal.* **2021**, *399*, 24–40. [[CrossRef](#)]
32. Samanta, C. Direct synthesis of hydrogen peroxide from hydrogen and oxygen: An overview of recent developments in the process. *Appl. Catal. A: Gen.* **2008**, *350*, 133. [[CrossRef](#)]

33. Choudhary, V.; Jana, P. Synergetic effect of two halogen promoters present in acidic reaction medium or catalyst on the H<sub>2</sub>O<sub>2</sub> formation (in H<sub>2</sub>-to-H<sub>2</sub>O<sub>2</sub> oxidation) and destruction over Pd/C (or Al<sub>2</sub>O<sub>3</sub>) catalyst. *J. Catal.* **2007**, *246*, 434–439. [[CrossRef](#)]
34. Choudhary, V.; Samanta, C. Role of chloride or bromide anions and protons for promoting the selective oxidation of H<sub>2</sub> by O<sub>2</sub> to H<sub>2</sub>O<sub>2</sub> over supported Pd catalysts in an aqueous medium. *J. Catal.* **2006**, *238*, 28–38. [[CrossRef](#)]
35. Han, Y.-F.; Lunsford, J.H. Direct formation of H<sub>2</sub>O<sub>2</sub> from H<sub>2</sub> and O<sub>2</sub> over a Pd/SiO<sub>2</sub> catalyst: The roles of the acid and the liquid phase. *J. Catal.* **2005**, *230*, 313–316. [[CrossRef](#)]
36. Gallina, G.; García-Serna, J.; Salmi, T.O.; Canu, P.; Biasi, P. Bromide and acids: A comprehensive study on their role on the hydrogen peroxide direct synthesis. *Ind. Eng. Chem. Res.* **2017**, *56*, 13367–13378. [[CrossRef](#)]
37. Choudhary, V.; Samanta, C.; Jana, P. Formation from direct oxidation of H<sub>2</sub> and destruction by decomposition/hydrogenation of H<sub>2</sub>O<sub>2</sub> over Pd/C catalyst in aqueous medium containing different acids and halide anions. *Appl. Catal. A-Gen.* **2007**, *317*, 234–243. [[CrossRef](#)]
38. Crole, D.A.; Freakley, S.J.; Edwards, J.K.; Hutchings, G.J. Direct synthesis of hydrogen peroxide in water at ambient temperature. *Proc. Math. Phys. Eng. Sci* **2016**, *472*, 20160156. [[CrossRef](#)]
39. Edwards, J.K.; Solsona, B.; Carley, A.F.; Herzing, A.A.; Kiely, C.J.; Hutchings, G.J. Switching off hydrogen peroxide hydrogenation in the direct synthesis process. *Science* **2009**, *323*, 1037–1041. [[CrossRef](#)] [[PubMed](#)]
40. Kim, J.; Chung, Y.-M.; Kang, S.-M.; Choi, C.-H.; Kim, B.-Y.; Kwon, Y.-T.; Kim, T.J.; Oh, S.-H.; Lee, C.-S. Palladium nanocatalysts immobilized on functionalized resin for the direct synthesis of hydrogen peroxide from hydrogen and oxygen. *ACS Catal.* **2012**, *2*, 1042–1048. [[CrossRef](#)]
41. Chung, Y.-M.; Kwon, Y.-T.; Kim, T.; Oh, S.-H.; Lee, C.-S. Direct synthesis of H<sub>2</sub>O<sub>2</sub> catalyzed by Pd nanoparticles encapsulated in the multi-layered polyelectrolyte nanoreactors on a charged sphere. *Chem. Commun. (Camb. Engl.)* **2011**, *47*, 5705–5707. [[CrossRef](#)]
42. Burato, C.; Campestrini, S.; Han, Y.-F.; Canton, P.; Centomo, P.; Canu, P.; Corain, B. Chemoselective and re-usable heterogeneous catalysts for the direct synthesis of hydrogen peroxide in the liquid phase under non-explosive conditions and in the absence of chemoselectivity enhancers. *Appl. Catal. A Gen.* **2009**, *358*, 224–231. [[CrossRef](#)]
43. Blanco-Brieva, G.; Desmedt, F.; Miquel, P.; Campos-Martin, J.M.; Fierro, J.L.G. Direct synthesis of hydrogen peroxide without the use of acids or halide promoters in dissolution. *Catal. Sci. Technol.* **2020**, *10*, 2333–2336. [[CrossRef](#)]
44. Deguchi, T.; Iwamoto, M. Catalytic properties of surface sites on Pd clusters for direct H<sub>2</sub>O<sub>2</sub> Synthesis from H<sub>2</sub> and O<sub>2</sub>: A DFT Study. *J. Phys. Chem. C* **2013**, *117*, 18540–18548. [[CrossRef](#)]